ISSN 1330-3651 (Print), ISSN 1848-6339 (Online)
UDC/UDK [620.172.21:519.87]:62-419

NURBS-IGA-BASED MODELLING: ANALYSIS AND OPTIMIZATION OF LAMINATED PLATES

Amir Behshad, Mohammad Reza Ghasemi

Original scientific paper
Analysis of the laminated composite plates under transverse loading is considered using the new method of Isogeometric Analysis (IGA). Non-Uniform Rational B-Splines (NURBS) are used as shape functions for modelling the geometry of the structure and are also used as shape functions in the analysis process. Boundary conditions are imposed using a kind of collocation method. To show robustness of the new technique, some examples are represented and are compared with the element free Galerkin and theoretical method at the end. The obtained results show the efficiency of the method. The optimization process is done using genetic algorithm method.

Keywords: *composite plates, genetic algorithm, isogeometric analysis, Non-Uniform Rational B-Splines (NURBS)*

Modeliranje temeljeno na NURGS-IGA metodi: analiza i optimalizacija laminatnih ploča

Izvorni znanstveni članak
Analiza laminatnih kompozitnih ploča izloženih poprečnom opterećenju razmatra se primjenom nove metode izogeometrijske analize (IGA). Non-Uniform Rational B-Splines (NURBS) koriste se kao funkcije oblika za modeliranje geometrije konstrukcije te također kao funkcije oblika u postupku analize. Granični uvjeti su zadani primjenom jedne vrste metode kolokacija. Izvrsnost se nove metode pokazuje na nekoliko primjera koji se uspoređuju s "Galerkin element free" metodom i teoretskom metodom na kraju. Dobiveni rezultati pokazuju učinkovitost nove metode. Postupak optimalizacije proveden je primjenom metode genetičkog algoritma.

Ključne riječi: *genetički algoritam, izogeometrijska analiza, kompozitne ploče, Non-Uniform Rational B-Splines (NURBS)*

1 Introduction

Isogeometric analysis (IGA) has been introduced by T. J. R. Hughes and co-authors in [1] as a novel technique for the discretization of partial differential equations in 2005. Isogeometric analysis is a computational mechanics technology based on functions used to represent geometry. The idea is to build a geometric model, e.g. through a computer aided design (CAD) system, and to directly use in the analysis, the functions describing the geometry, rather than approximating it through a finite element mesh. In CAD systems, non-uniform rational B-splines (NURBS) are the dominant technology. When a NURBS model is constructed, the basis functions used to define the geometry can be systematically enriched by *h*-, *p*-, or *k*-refinement (i.e., smooth order elevation) *without* altering the geometry or its parameterization. This means that mesh refinement techniques can be utilized without a link to the CAD database, in contrast with finite element methods. This appears to be a distinct advantage of isogeometric analysis over finite element analysis. In addition, on a per degree-of-freedom basis, isogeometric analysis has exhibited superior accuracy and robustness compared with finite element analysis. This is particularly true when a *k*-refined basis is adopted. In this case, the upper part of the discrete spectrum shows a much better behaviour, resulting in better conditioned discrete systems. It appears that isogeometric analysis offers several important advantages over classical finite element analysis.

IGA is having a growing impact on several fields, from fluid dynamics [2, 3], to structural mechanics [4, 5, 6, 7] and electromagnetics [8, 9]. A comprehensive reference for IGA is the book [10]. IGA methodologies are designed with the aim of improving the interoperability between numerical simulation of physical phenomena and the Computer Aided Design (CAD) systems. Indeed, the ultimate goal is to drastically reduce the error in the representation of the computational domain and the re-meshing by the use of the "exact" CAD geometry directly at the coarsest level of discretization. This is achieved by using B-Splines or Nun-Uniform Rational B-Splines (NURBS) for the geometry description as well as for the representation of the unknown fields. The use of Spline or NURBS functions, together with isoparametric concepts, results in an extremely successful idea and paves the way to many new numerical schemes enjoying features that would be extremely hard to achieve within a standard Finite Element Method (FEM). Splines and NURBS offer a flexible set of basis functions for which refinement, de-refinement, degree elevation and mesh deformation are very efficient (e.g., [6]).

Laminated composites plates exhibit a considerable variation in their material properties due to involvement of number of parameters that cannot be controlled effectively during fabrication. Randomness in several factors such as fibre orientation, volume fraction, fibre-matrix interface, and curing parameters is inherent in such laminated composite plates. Despite these uncertainties, their use in engineering applications has gained increasing popularity in recent years due to advantages like weight reduction (high strength/stiffness to weight ratio), longer life (no corrosion, low wear), fatigue endurance, and inherent damping. These plates are commonly employed in engineering applications as thin plates.

Finding an efficient composite structural design that meets requirements of a certain application can be achieved not only by sizing the cross-sectional areas and member thicknesses, but also by global or local tailoring of the material properties through selective use of orientation, number, and stacking sequence of lamina that

make up the composite laminate. The possibility of achieving an efficient design that is safe against multiple failure mechanisms, coupled with the difficulty in selecting the values of a large set of design variables makes structural optimization an efficient tool for the design of laminated composite structures. As an alternative to the conventional mathematical approaches, the meta-heuristic optimization techniques (genetic algorithm, ant colony optimization, particle swarm optimization, taboo search, etc.) have been used to obtain global or near global optimum solutions [11]. A genetic algorithm revolves the genetic evolution process and "survival of the fittest" strategy. It starts with an initial population of solutions, and the fitness value of each solution is evaluated such that the solution with higher fitness has higher chance to be reproduced for a mating pool. Then, the crossover operation and the mutation operation are performed on the mating parent pool to produce offspring. Each generation is continued to create until stop criteria are satisfied.

For the first time, Callahan and Weeks [12] applied genetic algorithm (GA) to demonstrate that GA can be a viable alternative to traditional search procedures in the design of composite laminates. Kogiso et al. [13] used GA with local improvement to optimize a laminated composite plate for buckling load maximization. Many others utilized this method or the modified type to optimize strength-to-weight ratio or other parameters [14 ÷ 16].

In contrast with other papers considering laminated plates, in this paper at first stage, modelling of the plate is done accurately using NURBS functions, then analysis process is done using the shape functions of first stage. Classical analysis methods like finite element, impose their chosen solution space onto the description of the geometry, but isogeometric analysis begins with a basis capable of representing the exact geometry and imposes it on the solution fields.

This paper is organized as follows: In Section 2 formulation of isogeometric method for analysing laminated plates is presented. NURBS basis functions are described, then weak form of the equilibrium equation for laminated plates is obtained based on the Hamilton principle. Boundary conditions are imposed by applying a kind of collocation method. This technique is given in Section 3. In Section 4.1 multi-objective optimization of laminated plates is explained using a relevant objective function with suitable constraints. Genetics algorithm, which is a powerful optimization method, is described in Section 4.2. Section 5 is devoted for representation of some examples to show robustness of the proposed method. In Section 6, the unique contributions of the paper, practical implications, and limitations are highlighted.

2 Isogeometric analysis formulation

NURBS are a standard tool for describing and modeling curves and surfaces in computer aided design and computer graphics (see Piegl and Tiller [17] and Rogers [18] for an extensive description of these functions and of their properties). In IGA method, NURBS are used as a basis functions in the analysis process. In the following we present a summary of the main features of isogeometric analysis.

- A mesh for a NURBS patch is defined by the product of knot vectors.
- Knot spans subdivide the domain into "elements".
- The support of each basis function consists of a small number of elements.
- The control points associated with the basis functions define the geometry.
- The isoparametric concept is invoked, that is, the unknown variables are represented in terms of a basis functions which define the geometry. The coefficients of a basis functions are the degrees-of-freedom, or *control variables*.
- Three different mesh refinement strategies are possible: analogues of classical *h*-refinement (by knot insertion) and *p*-refinement (by order elevation of the basis functions), and a new possibility referred to as *k*-refinement, which increases smoothness in addition to order.
- The element arrays constructed from isoparametric NURBS can be assembled into global arrays in the same way as finite elements.
- Dirichlet boundary conditions are applied to the control variables, in the same way as in finite elements. Neumann boundary conditions are satisfied naturally as in standard finite element formulations.

Generally, a NURBS curve of order p is defined as:

$$X(\xi)=\sum_{i=1}^{n} R_{i,p}(\xi)B_i, \tag{1}$$

$$R_{i,p}(\xi)=\frac{N_{i,p}(\xi)W_i}{\sum_{i=1}^{n} N_{i,p}(\xi)W_i}. \tag{2}$$

$R_{i,p}$ stands for the univariate NURBS basis functions, $B_i\,B_i$ are a set of n control points, W_i are a set of n weights corresponding to the control points that must be non-negative and $N_{i,p}$ represents the B-spline basis function of order p, to construct a set of n B-spline basis functions of order p, a knot vector is defined in a parametric space as follows:

$$\boldsymbol{\Xi}=\left\{\xi_1\ \ \xi_2\ \cdots\ \xi_{n+p+1}\right\}\ \ \xi_i\le\xi_{i+1}, i=1,2,\ldots,n+p. \tag{3}$$

The knot vectors used for analysis purposes are generally open knot vectors to satisfy the Kronecker-delta property at boundary points. In an open knot vector, the first and last knots are repeated $p+1$ times. Given a knot vector, the univariate B-spline basis function $N_{i,p}$ can be constructed by the following Cox-de Boor recursive formula.

$$N_{i,0}(\xi)=\begin{cases}1 \text{ if } \ \xi_i\le\xi\le\xi_{i+1}\\ 0\ \ otherwise\end{cases},$$
$$N_{i,p}(\xi)=\frac{\xi-\xi_i}{\xi_{i+p}-\xi_i}N_{i,p-1}(\xi)+\frac{\xi_{i+p+1}-\xi}{\xi_{i+p+1}-\xi_{i+1}}N_{i+1,p-1}(\xi), \tag{4}$$

Generally, a NURBS surface of order p in ξ direction and order q in η direction can be expressed as:

$$S(\xi,\eta)=\sum_{i=1}^{n}\sum_{j=1}^{m}R_{i,j}^{p,q}(\xi,\eta)B_{i,j},$$
$$R_{i,j}^{p,q}(\xi,\eta)=\frac{N_{i,p}(\xi)M_{j,q}(\eta)W_{i,j}}{\sum_{i=1}^{n}\sum_{j=1}^{m}N_{i,p}(\xi)M_{j,q}(\eta)W_{i,j}}. \quad (5)$$

$R_{i,j}^{p,q}$ stand for the bivariate NURBS basis functions. Quadratic B-spline basis functions are shown in Fig. 1.

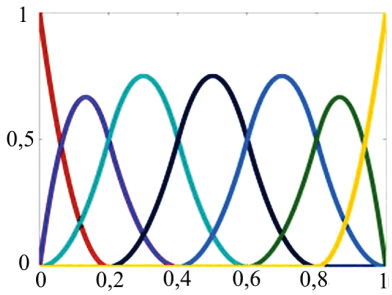

Figure1 Quadratic basis functions for an open knot vector Ξ ={0; 0; 0; 0,2; 0,4; 0,6; 0,8; 1; 1; 1}

Based on the classical thin plate theory, only the deflection of the plate w is chosen as the independent variable, while the other two displacement components u and v can be obtained from w. Therefore, the NURBS basis is employed for both the parameterization of the geometry and the approximation of the deflection field w as follows:

$$w(x(\xi))=\sum_{i=1}^{n\times m}\phi_i(\xi)w_i, \quad (6)$$

$$x(\xi)=\sum_{i=1}^{n\times m}\phi_i(\xi)B_i. \quad (7)$$

$\xi=(\xi,\eta)$ is the parametric coordinates vector, $x=(x,y)$ is the physical coordinates vector, B_i represents the control points of a $n\times m$ control mesh, w_i represents the deflection field at each control point, and $\phi_i(\xi)$ are the bivariate basis functions of order p and q, respectively.

A composite laminate with thickness h under transversally concentrated loading is shown in Fig. 1. The reference plane, z = 0, is located at the undeformed neutral plane of the laminated plate. The direction of fibres in a layer is indicated by α, Fig. 2.

A composite laminate with thickness h under transversally concentrated loading is considered. The reference plane, z = 0, is located at the undeformed neutral plane of the laminated plate. The direction of fibres in a layer is indicated by α. The bending strain energy of the laminates is written as:

$$\Pi_{\mathrm{b}}=\frac{1}{2}\int_{A}\boldsymbol{\varepsilon}_{\mathrm{p}}^{\mathrm{T}}\boldsymbol{\sigma}_{\mathrm{p}}\,\mathrm{d}A, \quad (8)$$

where A stands for the area of the plate, $\boldsymbol{\varepsilon}_{\mathrm{p}}$ is the pseudo-strain, and $\boldsymbol{\sigma}_{\mathrm{p}}$ is the pseudo-stress. For analysing thin composite laminates, the Classical Lamination Theory (CLT) has been used. CLT assumes that normal to the neutral surface of undeformed plate remains straight and normal to the neutral surface during deformation, which results in [19]:

$$\varepsilon_{xz}=0,\ \varepsilon_{yz}=0. \quad (9)$$

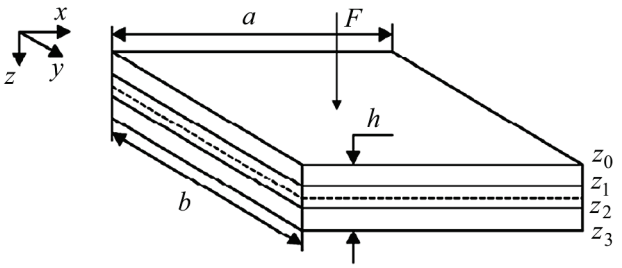

Figure 2a A laminated plate under transverse loading

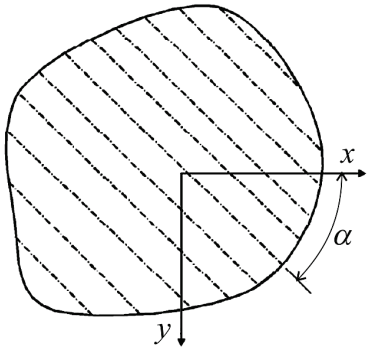

Figure 2b Fibre orientation in a laminate

So, only ε_x, ε_y and ε_{xy} are computed, and thus, the equations of plain stress are applied. Displacements in the x and y directions, u and, v at a distance z, from the neutral surface, can be expressed by:

$$u=-z\frac{\partial w}{\partial x},\ v=-z\frac{\partial w}{\partial y}. \quad (10)$$

Here, w is the deflection of the middle plane of the plate in the z direction. Using the above equations, one can write:

$$u=\begin{bmatrix}u & v & w\end{bmatrix}^{\mathrm{T}}=\begin{bmatrix}-z\frac{\partial}{\partial x} & -z\frac{\partial}{\partial y} & 1\end{bmatrix}^{\mathrm{T}}w=L_u. \quad (11)$$

The relationship between the three components of strain and the deflection can be given by:

$$\varepsilon_x=\frac{\partial u}{\partial x}=-z\frac{\partial^2 w}{\partial x^2},\ \varepsilon_y=\frac{\partial v}{\partial y}=-z\frac{\partial^2 w}{\partial y^2},$$
$$\varepsilon_{xy}=\frac{\partial u}{\partial x}+\frac{\partial v}{\partial y}=-2z\frac{\partial^2 w}{\partial x\partial y}, \quad (12)$$

or, in matrix form,

$$\boldsymbol{\varepsilon}=z\boldsymbol{L}w, \quad (13)$$

where $\boldsymbol{\varepsilon}$ is the vector of in-plane strains, and $\boldsymbol{L}$ is the differential operator vector given by:

$$\boldsymbol{L}=\left[-\frac{\partial^2}{\partial x^2}\quad -\frac{\partial^2}{\partial y^2}\quad -\frac{\partial^2}{\partial x\partial y}\right]^{\mathrm{T}}. \tag{14}$$

Pseudo-strains and pseudo-stresses are defined by:

$$\boldsymbol{\varepsilon}_{\mathrm{p}}=\boldsymbol{L}\boldsymbol{w},\ \boldsymbol{\sigma}_{\mathrm{p}}=\boldsymbol{D}\boldsymbol{\varepsilon}_{\mathrm{p}}=\boldsymbol{D}\boldsymbol{L}\boldsymbol{w}, \tag{15}$$

in which, $\boldsymbol{D}$ is the property matrix of materials. Based on the Hamilton principle, the equilibrium equation for a 2D solid mechanics can be written in the form [20]:

$$\boldsymbol{L}^{\mathrm{T}}\boldsymbol{\sigma}+\boldsymbol{b}=0, \tag{16}$$

where L is the differential operator, σ is the stress tensor and, $\boldsymbol{b}$ is the body force vector. The weak form can be given by:

$$\int_{\Omega}\delta\boldsymbol{\varepsilon}^{\mathrm{T}}\boldsymbol{\sigma}\,\mathrm{d}\Omega-\int_{\Omega}\delta\boldsymbol{w}^{\mathrm{T}}\boldsymbol{b}\,\mathrm{d}\Omega-\int_{\Gamma_t}\delta\boldsymbol{w}^{\mathrm{T}}\boldsymbol{t}\,\mathrm{d}\Gamma=0, \tag{17}$$

$$\int_{\Omega}\delta(\boldsymbol{L}\boldsymbol{w})^{\mathrm{T}}(\boldsymbol{D}\boldsymbol{L}\boldsymbol{w})\,\mathrm{d}\Omega-\int_{\Omega}\delta\boldsymbol{w}^{\mathrm{T}}\boldsymbol{b}\,\mathrm{d}\Omega-\int_{\Gamma_t}\delta\boldsymbol{w}^{\mathrm{T}}\boldsymbol{t}\,\mathrm{d}\Gamma=0, \tag{18}$$

in which $\boldsymbol{b}$ is the body force, $\boldsymbol{t}$ is the traction force, Ω is the problem domain, and Γ_t stands for the boundary of the solids on which traction forces are prescribed. The first term in (17) is the strain energy, the second and third terms are used to define works done by the external forces. As mentioned before, for displacement $\boldsymbol{w}$ one can write:

$$\boldsymbol{w}^h(x(\xi))=\sum_{i=1}^{n\times m}\boldsymbol{\phi}_i(\xi)w_i. \tag{19}$$

By using (19), the product of $\boldsymbol{L}\boldsymbol{w}$ (which gives the strain) becomes:

$$\boldsymbol{L}\boldsymbol{w}\approx\boldsymbol{L}\boldsymbol{w}^h=L\sum_{i=1}^{n\times m}\boldsymbol{\phi}_i(\xi)w_i=\sum_{i=1}^{n\times m}\underbrace{L\varphi_i(\xi)}_{B_i}w_i=\sum_{i=1}^{n\times m}B_iw_i. \tag{20}$$

Substituting (19) and (20) into (18) results in:

$$\begin{aligned}&\int_{\Omega}\delta\left(\sum_{i=1}^{n\times m}B_iw_i\right)^{\mathrm{T}}\left(\boldsymbol{D}\sum_{j=1}^{n\times m}B_jw_j\right)\mathrm{d}\Omega-\\&-\int_{\Omega}\delta\left(\sum_{i=1}^{n\times m}\varphi_iw_i\right)^{\mathrm{T}}\boldsymbol{b}\,\mathrm{d}\Omega-\int_{\Gamma_t}\delta\left(\sum_{i=1}^{n\times m}\varphi_iw_i\right)^{\mathrm{T}}\boldsymbol{t}\,\mathrm{d}\Gamma=0,\end{aligned} \tag{21}$$

Let us look at the first term in the above equation:

$$\begin{aligned}&\int_{\Omega}\delta\left(\sum_{i=1}^{n\times m}B_iw_i\right)^{\mathrm{T}}\left(\boldsymbol{D}\sum_{j=1}^{n\times m}B_jw_j\right)\mathrm{d}\Omega=\\&=\int_{\Omega}\delta\left(\sum_{i=1}^{n\times m}B_i^{\mathrm{T}}w_i^{\mathrm{T}}\right)\left(\boldsymbol{D}\sum_{j=1}^{n\times m}B_jw_j\right)\mathrm{d}\Omega.\end{aligned} \tag{22}$$

It should be noted that the summation, integration, and variation are all linear operators and therefore, they are exchangeable. Hence:

$$\begin{aligned}&\int_{\Omega}\delta\left(\sum_{i=1}^{n\times m}B_i^{\mathrm{T}}w_i^{\mathrm{T}}\right)\left(\boldsymbol{D}\sum_{j=1}^{n\times m}B_jw_j\right)\mathrm{d}\Omega=\\&=\sum_{i=1}^{n}\sum_{j=1}^{m}\delta w_i^{\mathrm{T}}\underbrace{\int_{\Omega}B_i^{\mathrm{T}}\boldsymbol{D}B_j\mathrm{d}\Omega}_{k_{ij}}w_i=\delta\boldsymbol{w}^{\mathrm{T}}\boldsymbol{K}\boldsymbol{w}.\end{aligned} \tag{23}$$

In above equation, k_{ij} is the element stiffness matrix, and K is the global stiffness matrix assembled using the element stiffness matrices. Next, let us examine the second term in (21).

$$\begin{aligned}&\int_{\Omega}\delta\left(\sum_{I}^{n\times m}\Phi_Iw_I\right)^{\mathrm{T}}\boldsymbol{b}\,\mathrm{d}\Omega=\sum_{I}^{n\times m}\delta w_I^{\mathrm{T}}\underbrace{\int_{\Omega}\Phi_I^{\mathrm{T}}b\,\mathrm{d}\Omega}_{f_I}=\\&=\sum_{I}^{n\times m}\delta w_I^{\mathrm{T}}f_I=\delta\boldsymbol{w}^{\mathrm{T}}F,\end{aligned} \tag{24}$$

where $\boldsymbol{f}_i$ is the force vector and $\boldsymbol{F}$ is the global force. The treatment for the third term in Eq. (21) is exactly the same as that for the second term, except that the body force vector is replaced by the traction vector. Therefore, the additional force vector can be given as:

$$t_i=\int_{\Gamma_t}\varphi_i^{\mathrm{T}}\bar{t}\,\mathrm{d}\Gamma. \tag{25}$$

Finally, summarizing Eqs. (22) ÷ (25), gives:

$$\begin{aligned}&\underbrace{\int_{\Omega}\delta\left(\sum_{i=1}^{n\times m}B_iw_i\right)^{\mathrm{T}}\left(\boldsymbol{D}\sum_{j=1}^{n\times m}B_jw_j\right)\mathrm{d}\Omega}_{\delta\boldsymbol{w}^{\mathrm{T}}\boldsymbol{K}\boldsymbol{w}}-\\&\underbrace{-\int_{\Omega}\delta\left(\sum_{i=1}^{n\times m}\varphi_iw_i\right)^{\mathrm{T}}\boldsymbol{b}\,\mathrm{d}\Omega-\int_{\Gamma_t}\delta\left(\sum_{i=1}^{n\times m}\varphi_iw_i\right)^{\mathrm{T}}\boldsymbol{t}\,\mathrm{d}\Gamma}_{\delta\boldsymbol{w}^{\mathrm{T}}\boldsymbol{F}}=0,\end{aligned} \tag{26}$$

which, results in:

$$\delta\boldsymbol{w}^{\mathrm{T}}\left(\boldsymbol{K}\boldsymbol{w}-\boldsymbol{F}\right)=0. \tag{27}$$

Because $\delta\boldsymbol{w}$ is arbitrary, the above equation can be satisfied only if:

$$\boldsymbol{K}\boldsymbol{w}-\boldsymbol{F}=0\Rightarrow\boldsymbol{K}\boldsymbol{w}=\boldsymbol{F}, \tag{28}$$

$$\begin{aligned}k_{ij}=\int_{\Omega}\Bigg[&D_{11}\frac{\partial^2\varphi_i}{\partial x^2}\frac{\partial^2\varphi_j}{\partial x^2}+\\&+D_{12}\left(\frac{\partial^2\varphi_i}{\partial x^2}\frac{\partial^2\varphi_j}{\partial y^2}+\frac{\partial^2\varphi_j}{\partial x^2}\frac{\partial^2\varphi_i}{\partial y^2}\right)+\\&+D_{22}\frac{\partial^2\varphi_i}{\partial y^2}\frac{\partial^2\varphi_j}{\partial y^2}+4D_{66}\frac{\partial^2\varphi_i}{\partial x\partial y}\frac{\partial^2\varphi_j}{\partial x\partial y}+\\&+2D_{16}\left(\frac{\partial^2\varphi_i}{\partial x^2}\frac{\partial^2\varphi_j}{\partial x\partial y}+\frac{\partial^2\varphi_j}{\partial y^2}\frac{\partial^2\varphi_i}{\partial x\partial y}\right)+\\&+2D_{26}\left(\frac{\partial^2\varphi_i}{\partial y^2}\frac{\partial^2\varphi_j}{\partial x\partial y}+\frac{\partial^2\varphi_j}{\partial y^2}\frac{\partial^2\varphi_i}{\partial x\partial y}\right)\Bigg]\mathrm{d}\Omega.\end{aligned} \tag{29}$$

For isotropic plates, stiffness matrix has a simpler form:

$$\begin{aligned}K_{ij}=\frac{\boldsymbol{D}}{2}\int_{\Omega}\Bigg[&2\left(\frac{\partial^2\varphi_i}{\partial x^2}+\frac{\partial^2\varphi_i}{\partial y^2}\right)\left(\frac{\partial^2\varphi_j}{\partial x^2}+\frac{\partial^2\varphi_j}{\partial y^2}\right)-\\&-2(1-\nu)\left(\frac{\partial^2\varphi_i}{\partial x^2}\frac{\partial^2\varphi_j}{\partial y^2}+\frac{\partial^2\varphi_j}{\partial x^2}\frac{\partial^2\varphi_j}{\partial y^2}-2\frac{\partial^2\varphi_i}{\partial x\partial y}\frac{\partial^2\varphi_j}{\partial x\partial y}\right)\Bigg]\mathrm{d}\Omega.\end{aligned} \tag{30}$$

3 Enforcing boundary conditions

The application of boundary conditions has been a difficult case, the details of which may be found in [21, 22]. One simple approach is a collocation method by which conditions are enforced exactly at a discrete set of boundary points. This is usually accomplished by replacing rows of the matrix equations resulted from discretization of the weak form with equations, which ensure the enforcement of boundary conditions.

Degrees of Freedom (DOF) of the structure can be categorized into two groups; constrained DOF, D_c, and unconstrained DOF, D_f. The partition of displacement and force vectors can be written as:

$$\boldsymbol{w}=\begin{Bmatrix}w_f\\w_c\end{Bmatrix},\ \boldsymbol{F}=\begin{Bmatrix}f_f\\f_c\end{Bmatrix}. \tag{31}$$

And, the stiffness matrix $\boldsymbol{K}$ and the shape function matrix $\boldsymbol{\Phi}$ are partitioned as:

$$\boldsymbol{K}=\begin{bmatrix}k_{ff}&k_{fc}\\k_{cf}&k_{cc}\end{bmatrix},\ \boldsymbol{\Phi}=\begin{bmatrix}\phi_{ff}&\phi_{fc}\\\phi_{cf}&\phi_{cc}\end{bmatrix}. \tag{32}$$

Then (28) can be written in the following form:

$$\begin{bmatrix}k_{ff}&k_{fc}\\k_{cf}&k_{cc}\end{bmatrix}\begin{Bmatrix}w_f\\w_c\end{Bmatrix}=\begin{Bmatrix}f_f\\f_c\end{Bmatrix}, \tag{33}$$

$$\begin{Bmatrix}w_f^h\\w_c^h\end{Bmatrix}=\begin{bmatrix}\phi_{ff}&\phi_{fc}\\\phi_{cf}&\phi_{cc}\end{bmatrix}\begin{Bmatrix}w_f\\w_c\end{Bmatrix}. \tag{34}$$

To enforce boundary conditions, second rows of (33) which are related to boundary points, are replaced by second rows of (34) in the following form:

$$\begin{bmatrix}k_{ff}&k_{fc}\\\phi_{cf}&\phi_{cc}\end{bmatrix}\begin{Bmatrix}w_f\\w_c\end{Bmatrix}=\begin{Bmatrix}f_f\\w_c^h\end{Bmatrix}. \tag{35}$$

4 Optimization process

4.1 Multi-objective optimization

A structural multi-objective optimization problem could be defined as:

$$\min\ F(x):=(f_1(x),f_n(x)), \tag{36}$$

where n is the number of objective functions and $F(x)$ is a k-dimensional vector of objective functions. There are some standard methods for dealing with multi-objective optimization problems, such as the Weighted Sum Method, Weighted Min-Max Method, Global Criterion Method, Bounded Objective Function Method, Lexicographic Method and Goal Programming Method [23 ÷ 26].

In recent years, using laminated composite materials in fabrication of mechanical, airspace, marine and machine industries is of major concern, due to their high strength and light weight. The multi-objective function introduced here consists of weight, cost and maximum moments. Thus, the weight and the cost will be minimized, while the moment for all the laminated plies is to be maximized. The design variables could be any combination of thickness, orientation of fibres and the material for each layer. The design parameters are angle of fibres (θ), layer thickness size (t) and material types (m) for each layer. The multi-objective function used contains three major terms, as in (37):

$$\begin{aligned}G=&\left(1+\frac{W}{W_{\max}}\right)^2+\Bigg[\left(1+\frac{C}{C_{\max}}\right)^2+\left(1+\frac{M_x}{M_x^*}\right)^2+\\&+\left(1+\frac{M_y}{M_y^*}\right)^2+\left(1+\frac{M_{xy}}{M_{xy}^*}\right)^2\Bigg]\cdot\frac{1}{R},\end{aligned} \tag{37}$$

where G is the goal function, W is weight of all layers, $W_{\max}$ is the maximum weight that layers can possess, C is cost of all layers, $C_{\max}$ is the maximum cost that layers may contain, M_x, M_y, M_{xy} are failure moments for all layers, M_x^*, M_y^*, M_{xy}^* are maximum moments caused by laterally concentrated loading on the laminated composite plate computed by the IGA method, and R is number of moments applied to the structure. For example, if only M_x^* and M_y^* are applied to the plate, then $R = 2$. Computation of the fixed value $W_{\max}$ was made by

choosing maximum thickness and heaviest material for all layers [27]. Similarly, C_{max} was computed by assigning the maximum thickness, and relatively most expensive material for all layers will be the case when $\theta = 45°$.

To enable a rather faster convergence to the optimum solution, some constraints are introduced. Thus, after the process of analysis of each individual belongs to each generation, if any of the designs had failure moments less than maximum computed moments and greater than 1,4 times of maximum computed moments, or being heavier than 45 % of maximum weight or found to be more expensive than 45 % of maximum cost of the plate, they will not be allowed to breed and will automatically be replaced by another randomly generated individual which satisfies all the constrains, as listed in (38):

$$\begin{cases} C \le 0{,}45 C_{\max} \\ w \le 0{,}45 w_{\max} \\ M^* \le M \le 1{,}4 M^* \end{cases}. \tag{38}$$

A catalogue list of 12 fibre angles, 13 layer thicknesses and 15 material types is introduced to the optimizer. The optimizer randomly chooses fibre angle, thickness, and material type for layers of the plate from the catalogue list to generate the first population. After generating the first population, and having analysed each of the individuals, the obtained objective values will be sorted. They are then credited with respect to their validities. After computing the objective value for the individuals, convergence criterion is investigated. There are two different methods for investigating convergence criterion in optimization process. The first ones are those which are related to the obtained results, and the second ones are those which are not related to the obtained results. In this research, Eq. (39) is used to control convergence criterion.

$$\left| \frac{(Fit)_{i\,\text{gen}} - (Fit)_{i\,\text{gen}-10}}{(Fit)_{i\,\text{gen}}} \right| \le \varepsilon, \ \varepsilon = 0{,}0001, \tag{39}$$

in which, $(Fit)_{i\,\text{gen}}$ is the objective value for generation i. It means that, if the objective value for generation i does not change considerably compared to the generation $i - 10$, then the optimization process will be terminated. Another convergence criterion used is related to maximum number of loops. In this research the maximum number of loops is assumed to be 50 which means that if the number of loops reaches 50 the process will be terminated either the convergence is occurred or not.

4.2 Genetic algorithm

In this research, we use genetic algorithm (GA) for a multi-objective optimization of laminated composite plates, where weight, cost and failure moments for the plates are interconnected. For the purpose of carrying the genetic operations then, a mating pool is generated. The procedure of generating the mating pool is such that: 100 % individuals in the mating pool= the first 50 % of total+ the first 20 % of total+ the first 10 % of total+ random 20 % of the remaining individuals [28]. Now, in order to proceed with creation of new generations towards better designs, genetic operators take place.

A. selection: due to a specific type of creating a mating pool, selection operator is carried out quite randomly where the credits to better designs were already given in generating the mating pool. However, out of a 100 % individuals in a generation, there are only 10 % of the new generation to be credited through selection.

B. cross-over: since the algorithm introduced in this study deals with real variables, which themselves are of three different types (θ, t, m), therefore, there will only be three positions for the cross-over to take place. Thus, when two designs are selected from mating pool, they may randomly exchange their θ, t or m. However, out of 100 % individuals in a generation, only 30 % of the new generation are to be created through cross-over.

C. mutation: this type of genetic operators is carried out similar to cross-over. In this case, variables (θ, t, m) of some individuals will be changed randomly, as a result of which children are created. However, out of 100 % individuals in a generation, there are 60 % of the new generation to be created through mutation.

5 Examples

Example 1. In this example, an exponential function, Eq. (40), is approximated using the NURBS shape functions, and the moving least square (MLS) shape functions which are used in the element free Galerkin method.

$$f(x) = \exp(-16 \times (x-4)^2 + 3). \tag{40}$$

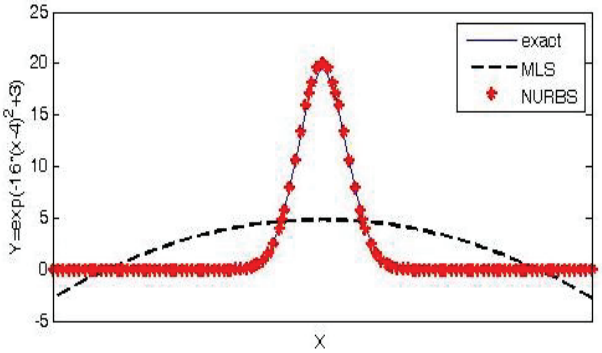

Figure 3 Function approximation with two methods of NURBS and MLS

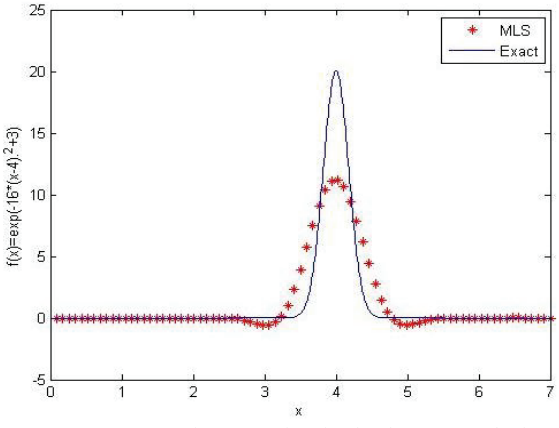

Figure 4 (a) Function approximation by the MLS method

As we can see, robustness of NURBS shape functions which are used in the IGA method is more powerful than MLS shape functions of the element free Galerkin (EFG) method.

In Figs. 4a and 4b, at first, the exponential function is approximated using MLS shape functions, then the same function is approximated using NURBS shape functions. We can see robustness of the NURBS functions in comparison with MLS shape functions of the element free Galerkin method.

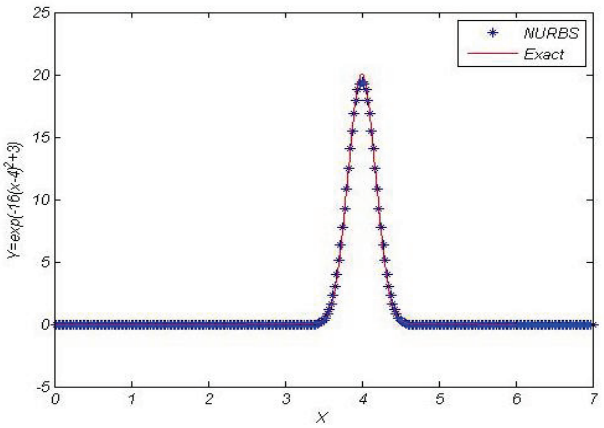

Figure 4 (b) Function approximation by the NURBS method

Example 2. This example is an isotropic rectangular plate, as in Fig. 5, with simply supported boundary conditions and uniform thickness h = 0,001 m, a length of 0,5 m, and a width equal to 0,25 m subjected to two laterally concentrated loads, $f_1 = f_2$ = 6500 N. The first load is applied at the point x = 0,250 m, y = 0,083 m, and the second load is applied at the point x = 0,250 m, y = 0,166 m. Young's modulus and Poisson's ratio are assumed to be $E = 2\times10^{10}$ N/m^2 (≈ 20 GPa) and ν = 0,3, respectively. The IGA method is used for the analysis process. The results are compared with those of the exact method to show the IGA robustness.

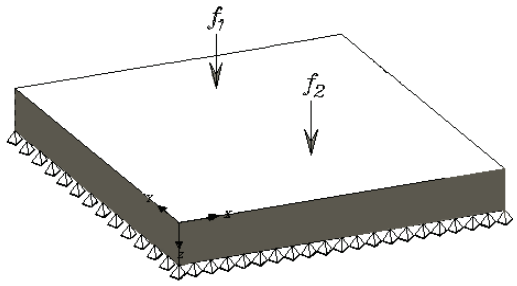

Figure 5 Plate related to example 2

The plate is modelled using NURBS shape functions. Deflections, pseudo strains, and pseudo stresses are calculated by the IGA method. The control points used to model the geometry, before refinement, are displayed in Fig. 6.

The degrees of NURBS shape functions in each direction are equal to 2. The knot vector in each direction is: Ξ = {0; 0; 0; 0,5; 1; 1; 1}. The results of deflection for $x \in$ [0; 0,5] and, y = 0,125 m are compared with exact method in Fig. 7. Compared with the exact results, good agreement has been achieved. Energy norm has been calculated using $q. (41). For this example, the energy norm was equal to e_e = 0,033211452. The energy norm computed by the element free Galerkin method for this problem was equal to e_e = 0,034197341. In comparison with element free Galerkin method, the energy norm computed by the isogeometric method is more reliable.

$$e_e = \sqrt{\left(\frac{1}{2}\int_{\Omega}\left(\varepsilon_{\text{Num}}-\varepsilon_{\text{Exact}}\right)^{\text{T}}\boldsymbol{D}\left(\varepsilon_{\text{Num}}-\varepsilon_{\text{Exact}}\right)\right)\text{d}\Omega}. \qquad (41)$$

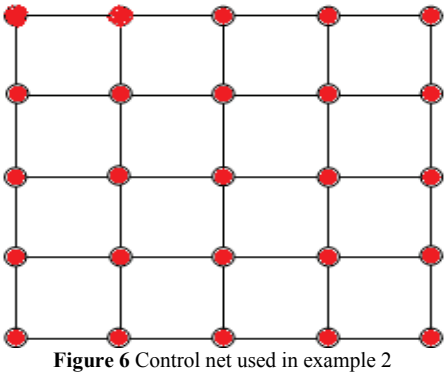

Figure 6 Control net used in example 2

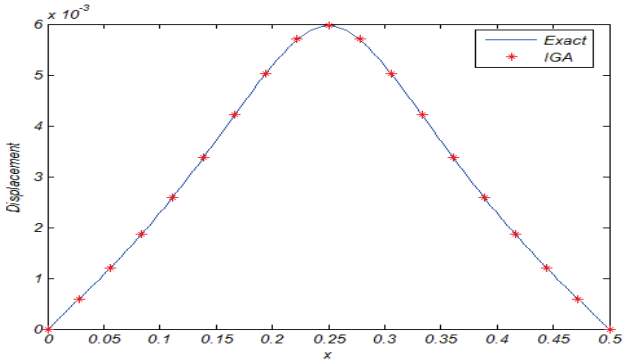

Figure 7 Deflection computed with the IGA and exact method

The results of deflection for $x \in$ [0; 0,5] and, y = 0,125 m compared with the results of element free Galerkin method are shown in Fig. 8. Compared with the exact results, accuracy of IGA results is better than the EFG ones.

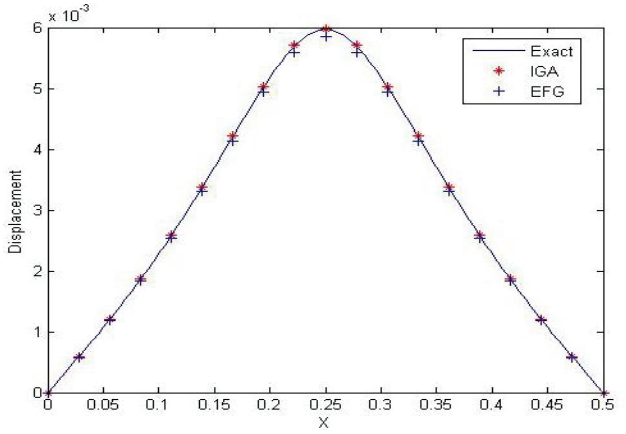

Figure 8 Deflection computed with the IGA, EFG and exact method

Example 3. This example is a laminated plate with 8 layers, four of which are symmetrical as shown in Tab. 1. The laminated plate is under five transversally concentrated loads, Fig. 9. The laminate is supported

simply at all edges. The loads are applied at the points as the following:

$$x_2 = \frac{a}{3}, y_2 = \frac{b}{5}, x_3 = \frac{3a}{4}, y_3 = \frac{b}{3}, x_4 = \frac{a}{3}, y_4 = \frac{2b}{3},$$
$$x_5 = \frac{3a}{5}, y_5 = \frac{4b}{5}, x_1 = \frac{a}{2}, y_1 = \frac{b}{2},$$

$f_1 = 20$ kN, $f_2 = 45$ kN, $f_3 = 20$ kN, $f_4 = 10$ kN, $f_5 = 5$ kN.

Ply angles, thicknesses and material types used for the layers are indicated in Tab. 1. IGA method is used for the analysis process. Moments computed by the IGA method, are shown in Tab. 1. The optimization is run using different initial population sizes of 15, 25, 35, 50 and 75, as indicated in Fig. 10.

Table 1 Parameters of laminates for Example 3

Layer No.	Angle, °	Thickness, m	Material
1(8)	−75	0,001	T300/5208
2(7)	60	0,0008	AS/3501
3(6)	45	0,0015	IM6/APC2
4(5)	90	0,0008	S2-449/SP
M_x^*	−2565,4321 N·m		
M_y^*	−11636,7876 N·m		
M_{xy}^*	1649,8732 N·m		

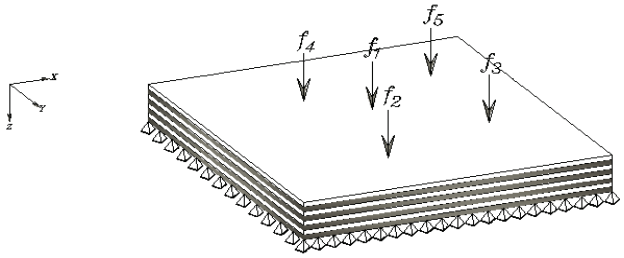

Figure 9 The laminate with 8 layers related to Example 3

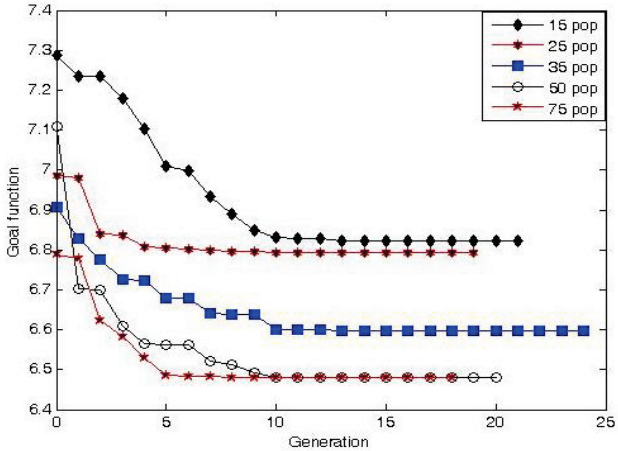

Figure 10 A convergence history of the multi-objective variations with different initial populations for Example 3

Tab. 2 indicates the optimum values obtained for the weight and cost of Example 3 for the case in which initial population is 50.

Table 2 Parameters of optimized laminates for Example 3

Layer No.	Angle, °	Thickness, m	Material
1(8)	90	0,0006	Generic Kevlar
2(7)	90	0,0008	AS4/5250-3
3(6)	−60	0,0006	Generic Kevlar
4(5)	0	0,001	Generic S-Glass
Goal function	6,481113		
Weight	196,48 kN		
Cost	10,139 U		
M_x	−2581,821 N·m		
M_y	−11656,64 N·m		
M_{xy}	1663,94 N·m		

6 Unique contributions, practical implications, and limitations

In this paper, analysis and optimization of laminated plates are done linking isogeometric analysis method and genetics algorithm optimization method for the first time. Geometry of the laminated plates is modelled exactly, in contrast with other methods in which geometry is approximated. Therefore, the obtained results are more reliable, and present greater precision and tighter integration of the overall modelling-analysis process. Without accurate geometry and mesh adaptivity, convergence and high-precision results are impossible. The benefits of design optimization have been largely unavoidable to industry. The bottleneck is that to do optimization, the geometry-to-mesh mapping needs to be automatic, differentiable, and tightly integrated with the solver and optimizer. The process requires simulations with numerous samples of models. Sampling puts a premium on the ability to rapidly generate geometry models, meshes and analyses, which again leads to the need for tightly integrated geometry, meshing, and analysis.

7 Conclusion

In this article, isogeometric analysis method is used to analyse laminated composite plates. The obtained results are compared with those of the exact method. Robustness and accuracy of the IGA method is shown perfectly. In the first example, we can see NURBS shape functions robustness in comparison with moving least square technique, which is used as shape function in the element free Galerkin method. At the third example, a laminated composite plate under transverse loading is analysed by the method of isogeometric analysis. The obtained results show the robustness and accuracy of the IGA method. At the end, the laminated plate is optimized using genetic algorithm. Future research could be conducted using modern heuristic methods like ant-colony, bee colony, particle swarm optimization methods as optimizer and isogeometric method as analyser.

8 References

[1] Thomas, H. JR; Cottrell, J. A.; Bazilevs, Y. Isogeometric analysis: CAD, finite elements, NURBS, exact geometry and mesh refinement. // Computer methods in applied mechanics and engineering 194, 39(2005), pp. 4135-4195.

[2] Bazilevs, Y.; Calo, V. M.; Hughes, T. J. R.; Zhang, Y. Isogeometric fluid-structure interaction: theory, algorithms, and computations. // Computational Mechanics. 43, 1(2008), pp. 3-37.
[3] Buffa, A.; De Falco, C.; Sangalli, G. Isogeometric analysis: new stable elements for the Stokes equation. // International Journal for Numerical Methods in Fluids. 1, (2000), pp. 1-15.
[4] Auricchio, F.; Beirão da Veiga, L.; Lovadina, C.; Reali, A. The importance of the exact satisfaction of the incompressibility constraint in nonlinear elasticity: mixed FEMs versus NURBS-based approximations. // Computer Methods in Applied Mechanics and Engineering. 199, 5(2010), pp. 314-323.
[5] Auricchio, F.; da Veiga, L. B.; Buffa, A.; Lovadina, C.; Reali, A.; Sangalli, G. A fully "locking-free" isogeometric approach for plane linear elasticity problems: a stream function formulation. // Computer methods in applied mechanics and engineering. 197, 1(2007), pp. 160-172.
[6] Benson, D. J.; Bazilevs, Y.; Hsu, M. C.; Hughes, T. J. R. Isogeometric shell analysis: the Reissner–Mindlin shell. // Computer Methods in Applied Mechanics and Engineering. 199, 5(2010), pp. 276-289.
[7] Lipton, S.; Evans, J. A.; Bazilevs, Y.; Elguedj, T.; Hughes, T. J. Robustness of isogeometric structural discretizations under severe mesh distortion. // Computer Methods in Applied Mechanics and Engineering. 199, 5(2010), pp. 357-373.
[8] Buffa, A.; Sangalli, G.; Vázquez, R. Isogeometric analysis in electromagnetics: B-splines approximation. // Computer Methods in Applied Mechanics and Engineering. 199, 17(2010), pp. 1143-1152.
[9] Buffa, A., Rivas, J., Sangalli, G., Vázquez, R. Isogeometric discrete differential forms in three dimensions. // SIAM Journal on Numerical Analysis, 49, 2(2011), pp. 818-844.
[10] Cottrell, J. A.; Hughes, T. J.; Bazilevs, Y. Isogeometric analysis: toward integration of CAD and FEA. John Wiley & Sons. (2009).
[11] Kaveh, A.; Hashemi Soudmand, B.; Sheikholeslami, R. optimal design of laminated composite structures via hybrid charged system search and particle swarm optimization. // Asian journal of civil engineering (Bhrc). 14, 4(2013), pp. 587-604.
[12] Callahan, K. J.; Weeks, G. E. Optimum design of composite laminates using genetic algorithms. // Composites Engineering. 2, (1992), pp. 149-60.
[13] Kogiso, N.; Watson, L. T.; Gurdal, Z.; Haftka, R. T. Genetic algorithm with local improvement for composite laminate design. // Structural and Multidisciplinary Optimization. 7, (1994), pp. 207-18.
[14] Soremekun, G.; Gurdal, Z.; Haftka, R. T.; Watson, L. T. Composite laminate design optimization by genetic algorithm with generalized elitist selection. // Computers and Structures. 79, (2001), pp. 131-43.
[15] Riche, R. L.; Haftka, R. T. Improved genetic algorithm for minimum thickness composite laminate design. // Composites Engineering. 5, (1994), pp. 143-61.
[16] Muelas, S.; Pena, J. M.; Robles, V.; Muzhetskaya, K.; LaTorre, A.; Miguel, P. D. Optimizing the design of composite Panels using an improved Genetic Algorithm. Proceedings of the International Conference on Engineering Optimization, Rio de Janeiro: Brazil, 2008.
[17] Piegl, L. A.; Tiller, W. The NURBS book. Springer, 1997.
[18] Rogers, D. F. An introduction to NURBS: with historical perspective. Morgan Kaufmann, 2001.
[19] Agarwal, B. D.; Broutman, L. J.; Chandrashekhara, K. Analysis and performance of fiber composites. Wiley.com, 2006.
[20] Liu, G. R. Mesh free methods: moving beyond the finite element method. CRC press, 2010.
[21] Wagner, G. J.; Liu, W. K. Application of essential boundary conditions in mesh-free methods: a corrected collocation method. // International Journal for Numerical Methods in Engineering. 47, 8(2000), pp. 1367-1379.
[22] Wu, C. K. C.; Plesha, M. E. Essential boundary condition enforcement in meshless methods: boundary flux collocation method. // International Journal for Numerical methods in engineering. 53, 3(2002), pp. 499-514.
[23] Haimes, Y. Y.; Freedman, H. T. Multiobjective optimization in water resources systems: the surrogate worth trade-off method (Vol. 3). Elsevier, 2011.
[24] Zeleny, M. Multiple criteria decision making (Vol. 25). J. L. Cochrane (Ed.). New York: McGraw-Hill, 1982.
[25] Cohon, J. L. Multiobjective programming and planning, Academic Press, New York, 2004.
[26] Fonseca, C. M.; Fleming, P. J. An overview of evolutionary algorithms in multiobjective optimization. // Evolutionary computation. 3, 1(1995), pp. 1-16.
[27] Soremekun, G. A. Genetic algorithms for composite laminate design and optimization (Doctoral dissertation, Virginia Polytechnic Institute and State University), 1997.
[28] Ghasemi, M. R.; Ehsani, A. A hybrid radial-based Neuro-GA multiobjective design of laminated composite plates under moisture and thermal actions. // International Journal of Computer, Information, and System Science, and Engineering. 1, 2(2007), pp. 110-117.

Authors' addresses

Amir Behshad
Faculty of Engineering, University of Sistan and Baluchestan, Zahedan, Iran
E-mail: amir.behshad@hotmail.com

Mohammad Reza Ghasemi *(corresponding author)*
Faculty of Engineering, University of Sistan and Baluchestan, Zahedan, Iran
E-mail: mrghasemi@hamoon.usb.ac.ir